INTERNATIONAL JOURNAL OF OPTIMIZATION IN CIVIL ENGINEERING
Int. J. Optim. Civil Eng., 2013; 3(4):575-600

OPTIMAL DESIGN OF SINGLE-LAYER BARREL VAULT FRAMES USING IMPROVED MAGNETIC CHARGED SYSTEM SEARCH

A. Kaveh*, †, 1, B. Mirzaei[2] and A. Jafarvand[2]

[1]*Centre of Excellence for Fundamental Studies in Structural Engineering, Iran University of Science and Technology, Narmak, Tehran-16, Iran*

[2]*Department of Civil Engineering, University of Zanjan, Zanjan, Iran*

ABSTRACT

The objective of this paper is to present an optimal design for single-layer barrel vault frames via improved magnetic charged system search (IMCSS) and open application programming interface (OAPI). The IMCSS algorithm is utilized as the optimization algorithm and the OAPI is used as an interface tool between analysis software and the programming language. In the proposed algorithm, magnetic charged system search (MCSS) and improved harmony search (IHS) are utilized to achieve a good convergence and good solutions especially in final iterations. The results confirm the efficiency of OAPI as a powerful interface tool in the analysis process of barrel vault structures and also the ability of IMCSS algorithm in fast convergence and achieving optimal results.

Received: 10 March 2013; Accepted: 20 September 2013

KEY WORDS: magnetic charged system search, improved harmony search, open application programming interface, optimal design, single layer barrel vault frame

1. INTRODUCTION

The popularity of barrel vaults is partly due to the economy of these types of space structures, and because all arches can be constructed as identical members. At the same time, their cylindrical shape provided a great deal of volume under the roof [1]. Braced

*Corresponding author: A. Kaveh, Centre of Excellence for Fundamental Studies in Structural Engineering, Iran University of Science and Technology, Tehran-16, Iran.

†E-mail address: alikaveh@iust.ac.ir (A. Kaveh)

barrel vaults are developable surfaces of zero Gauss curvature generated by the movement of a curve, known as the Directrix, over a generator straight line. This curve can be a circular arc, an ellipse, a catenary, a parabola or a cycloid [2]. The earlier types of constructed braced barrel vaults were single-layer structures.

There are several possible types of bracing which have been used in the construction of single-layer braced barrel vaults. The fully triangulated systems can theoretically be analysed as pin-connected structures. The barrel vaults, having the diagonal or hexagonal types of bracing, must have rigid joints to be stable and the influence of bending moments in their stress distribution is much more pronounced than in the other types. In general, the patterns of space grids can be characterized as two-way or three-way, depending on whether the members intersecting at a node run in two or three directions. From the single-layer barrel vaults analysed, the three-way grid type has proven to provide the most uniform stress distribution throughout the structure, and due to the low number of joints required in comparison with other configurations, should result in economical structural system [1, 3].

In the field of structural optimization, many meta-heuristic algorithms have been proposed in the last three decades. Each meta-heuristic approach consists of a group of search agents which explore the feasible region based on both randomization and some specified rules. The rules are usually inspired by natural phenomena laws. Recently, a new meta-heuristic algorithm has been proposed by Kaveh and Talatahari which is called Charged System Search (CSS) [4]. The CSS algorithm is based on the Coulomb and Gauss laws from physics and the governing laws of motion from the Newtonian mechanics. In this algorithm which can be considered as a multi-agent approach, each agent is a Charged Particle (CP). Each CP is considered as a charged sphere with a specified radius, having a uniform volume charge density which can insert an electric force to the other CPs. Afterwards, the CSS algorithm is modified to magnetic charged system search (MCSS) by Kaveh et al. [5]. In this algorithm, in addition to electrical force, the magnetic force is considered, and then the movements of CPs due to the total force (Lorentz force) are determined using Newtonian mechanical laws.

Although, there are many studies on optimization of truss structures using the current meta-heuristic algorithms, however, there are not many studies on optimization of space structures, and further studies on optimization of these spatial structures are needed. In the present study, optimal design of single layer barrel vault frames as a kind of space structures is performed. In this field, Kaveh and Eftekhar [6] have presented optimal design of barrel vault frames using IBB-BC algorithm, in which a 173-bar single layer barrel vault is optimized under both symmetrical and unsymmetrical load cases. In another study by Kaveh et al. [7] some single layer barrel vaults are optimized via CSS algorithm. In that paper [7], the stability of the barrel vaults are checked during the analysis to make sure that the structure does not lose its load carrying capacity due to instability.

In this paper, improved CSS and MCSS algorithms are proposed for optimal design of single layer barrel vault frames. In these algorithms, an improved harmony search scheme is utilized and some of the most effective parameters in the convergence rate of the algorithm are improved to achieve good convergence and more optimal results.

This paper is organized as follows: Section 2 presents the statement of the optimization design problem for barrel vault frames. In Section 3, the standard CSS and MCSS algorithms are reviewed, and the improved version of these algorithms are presented. Section 4 provides Open Application Programming Interface (OAPI) as a tool for structural analysis. In Section 5, the static loading conditions acting on the structures are described. Section 6 contains two illustrative numerical examples to determine the efficiency of the proposed algorithms, and finally the concluding remarks are derived in Section 7.

2. STATEMENT OF OPTIMIZATION PROBLEM FOR BARREL VAULT FRAMES

The purpose of size optimization of frame structures is to minimize the weight of the structure, W, through finding the optimal cross-sectional areas A_i of members, in which all constraints exerted on the problem must be satisfied, simultaneously. Thus, the optimal design of barrel vault frame structures can be formulated as:

$$\begin{array}{ll} \text{Find} & X = [x_1, x_2, x_3, \ldots, x_n] \\ \text{to minimize} & Mer(X) = f_{penalty}(X) \times W(X) \end{array} \tag{1}$$

Subjected to the following constraints

Displacement constraint:

$$\upsilon_i^d = \left|\frac{\delta_i}{\bar{\delta}_i}\right| - 1 \le 0, \quad i = 1,2,\ldots,nn \tag{2}$$

Shear constraint, for both major and minor axis (AISC-LRFD, Chapter G) [8]:

$$\upsilon_i^s = \frac{V_u}{\phi_v V_n} - 1 \le 0, \quad i = 1,2,\ldots,nm \tag{3}$$

Constraints corresponding to interaction of flexure and axial force (AISC-LRFD, Chapter H) [8]:

$$\upsilon_i^I = \begin{cases} \dfrac{P_u}{2\phi_c P_n} + \left(\dfrac{M_{ux}}{\phi_b M_{nx}} + \dfrac{M_{uy}}{\phi_b M_{ny}}\right) - 1 \le 0 & for\ \dfrac{P_u}{\phi_c P_n} < 0.2 \\ \dfrac{P_u}{\phi_c P_n} + \dfrac{8}{9}\left(\dfrac{M_{ux}}{\phi_b M_{nx}} + \dfrac{M_{uy}}{\phi_b M_{ny}}\right) - 1 \le 0 & for\ \dfrac{P_u}{\phi_c P_n} \ge 0.2 \end{cases}, \quad i = 1,2,\ldots,nm \tag{4}$$

where X is the vector containing the design variables; for the discrete optimum design problem, the variables x_i are selected from an allowable set of discrete values; n is the number of member groups; $Mer(X)$ is the merit function; $W(X)$ is the cost function, which is taken as the weight of the structure; $f_{penalty}(X)$ is the penalty function which results from the violations of the constraints corresponding to the response of the structure; nn is the number of nodes; δ_i, $\bar{\delta}_i$ are the displacement of the joints and the allowable displacement, respectively; nm is the number of members; V_u is the required shear strength; V_n is the nominal shear strength which is defined by the equations in Chapter G of the LRFD Specification [8]; ϕ_v is the shear resistance factor $\phi_v = 0.9$; P_u is the required strength (tension or compression); P_n is the nominal axial strength (tension or compression); ϕ_c is the resistance factor ($\phi_c = 0.9$ for tension, $\phi_c = 0.85$ for compression); M_u is the required flexural strength; i.e., the moment due to the total factored load (Subscript x or y denotes the axis about which bending occurs.); M_n is the nominal flexural strength determined in accordance with the appropriate equations in Chapter F of the LRFD Specification [8] and ϕ_b is the flexural resistance reduction factor ($\phi_b = 0.9$).

For the displacement limitations which must be considered to ensure the serviceability requirements, the BS 5950 [9] limits the vertical deflections δ_v due to unfactored loads to Span/360, i.e. $\delta_V = S/360$ and horizontal displacements δ_H to Height/300, i.e. $\delta_H = h/300$ [10].

The nominal axial strength P_n is defined as:

$$P_n = A_g F_{cr} \tag{5}$$

where A_g is the gross area of member and F_{cr} is obtained as follows

$$F_{cr} = \begin{cases} \left(0.658^{\lambda_c^2}\right).F_y & for\ \lambda_c \le 1.5 \\ \left(\dfrac{0.877}{\lambda_c^2}\right).F_y & for\ \lambda_c > 1.5 \end{cases} \tag{6}$$

where F_y is the specified minimum yield stress and the boundary between inelastic and elastic instability is $\lambda_c = 1.5$, where the parameter

$$\lambda_c = \frac{KL}{r\pi}\sqrt{\frac{F_y}{E}} \tag{7}$$

with K being the effective length factor for the member (*K = 1.0 for braced frames [8]*), L is the unbraced length of member, r is the governing radius of gyration about plane of buckling, and E is the modulus of elasticity for the member of structure.

The cost function can be expressed as:

$$W(X)=\sum_{i=1}^{nm}\gamma_i \cdot x_i \cdot L_i \tag{8}$$

where γ_i is the material density of member i; L_i is the length of member i; and x_i is the cross-sectional area of member i as the design variable.

The penalty function is used as in [11]:

$$f_{penalty}(X)=\left(1+\varepsilon_1 \cdot \sum_{j=1}^{np}\upsilon_{(j)}^{k}\right)^{\varepsilon_2}, \tag{9}$$

where np is the number of multiple loading conditions. In this paper ε_1 is taken as unity and ε_2 is set to 1.5 in the first iterations of the search process, but gradually it is increased to 3 [11]. υ^k is the summation of penalties for all imposed constraints for kth charged particle which is mathematically expressed as:

$$\upsilon=\sum_{i=1}^{nn}\max\left(\upsilon_i^d,0\right)+\sum_{i=1}^{nm}\left(\max\left(\upsilon_i^I,0\right)+\max\left(\upsilon_i^s,0\right)\right) \tag{10}$$

where υ_i^d, υ_i^I, υ_i^s are the summation of displacement, shear and interaction formula penalties, calculated by Eqs. (2) through (4), respectively.

3. THE OPTIMIZATION ALGORITHM

3.1 Introduction to CSS and MCSS

Recently, the CSS algorithm which is presented by Kaveh and Talathari [4] for optimization problems is modified to MCSS algorithm by Kaveh et al. [5]. The CSS algorithm takes its inspiration from the physic laws governing a group of CPs. These charge particles are sources of the electric fields, and each CP can exert electric force on other CPs. The movement of each CP due to the electric force can be determined using the Newtonian mechanic laws.

The MCSS algorithm uses the physic law which has proved that when a charged particle moves, produces a magnetic field, so this magnetic field can exert a magnetic force on other CPs. Thus, the CSS algorithm is modified to MCSS algorithm considering this force in addition to electric force.

The MCSS algorithm can be summarized as follows:

- **Level 1. Initialization**

Step 1: Initialization. Initialize CSS algorithm parameters; the initial positions of CPs are determined randomly in the search space

$$x_{i,j}^{(0)} = x_{i,min} + rand \cdot (x_{i.max} - x_{i,min}),\ i = 1, 2, ..., n. \tag{11}$$

where $x_{i,j}^{(0)}$ determines the initial value of the *i*th variable for the *j*th CP; $x_{i,min}$ and $x_{i,max}$ are the minimum and the maximum allowable values for the *i*th variable; *rand* is a random number in the interval [0,1]; and *n* is the number of variables. The initial velocities of charged particles are zero

$$v_{i,j}^{(0)} = 0,\ i = 1, 2, ..., n. \tag{12}$$

The magnitude of the charge is defined as follows:

$$q_i = \frac{\text{fit(i) - fitworst}}{\text{fitbest - fitworst}},\ i = 1, 2, ..., N. \tag{13}$$

where *fitbest* and *fitworst* are the best and the worst fitness of all particles; *fit(i)* represents the fitness of the agent *i*; and *N* is the total number of CPs. The separation distance r_{ij} between two charged particles is defined as:

$$r_{ij} = \frac{\|X_i - X_j\|}{\|(X_i + X_j)/2 - X_{best}\| + \varepsilon}, \tag{14}$$

where X_i and X_j are the positions of the *i*th and *j*th CPs, X_{best} is the position of the best current CP, and ε is a small positive number to avoid singularities.

Step 2. CP ranking. Evaluate the values of fitness function for the CPs, compare with each other and sort them in an increasing order.

Step 3. CM creation. Store CMS number of the first CPs and their related values of the objective function in the CM (based on CMS size).

- **Level 2: Search**

Step 1: Force determination.

The probability of the attraction of the *i*th CP by the *j*th CP is expressed as:

$$p_{ij} = \begin{cases} 1 & \dfrac{\text{fit(i) - fitbest}}{\text{fit(j) - fit(i)}} > rand \ \ or \ \ \text{fit(j)} > \text{fit(i)}, \\ 0 & \text{else.} \end{cases} \tag{15}$$

where *rand* is a random number which is uniformly distributed in the range of (0,1). The resultant electrical force $F_{E,j}$ acting on the *j*th CP can be calculated as follow:

$$F_{\mathrm{E,j}} = q_j \cdot \sum_{i,i \neq j} \left(\frac{q_i}{a^3} r_{ij} \cdot i_1 + \frac{q_i}{r_{ij}^{\ 2}} i_2 \right) \cdot p_{ij} (X_i - X_j), \quad \begin{cases} i_1 = 1, i_2 = 0 \Leftrightarrow r_{ij} < a, \\ i_1 = 0, i_2 = 1 \Leftrightarrow r_{ij} \geq a, \\ j = 1, 2, \ldots, N. \end{cases} \tag{16}$$

The probability of the magnetic influence (attracting or repelling) of the *i*th wire (CP) on the *j*th CP is expressed as:

$$pm_{\mathrm{ij}} = \begin{cases} 1 & \mathrm{fit(j) > fit(i)}, \\ 0 & \mathrm{else.} \end{cases} \tag{17}$$

where *fit(i)* and *fit(j)* are the objective values of the *i*th and *j*th CP, respectively. This probability determines that only a good CP can affect a bad CP by the magnetic force.
The resultant magnetic force $F_{B,j}$ acting on the *j*th CP due to the magnetic field of the *i*th virtual wire (*i*th CP) can be expressed as:

$$F_{\mathrm{B,j}} = q_j \cdot \sum_{i,i \neq j} \left(\frac{I_i}{R^2} r_{ij} \cdot z_1 + \frac{I_i}{r_{ij}} \cdot z_2 \right) \cdot pm_{ij} (X_i - X_j), \quad \begin{cases} z_1 = 1, z_2 = 0 \Leftrightarrow r_{ij} < R, \\ z_1 = 0, z_2 = 1 \Leftrightarrow r_{ij} \geq R, \\ j = 1, 2, \ldots, N. \end{cases} \tag{18}$$

where q_i is the charge of the *i*th CP, R is the radius of the virtual wires, I_i is the average electric current in each wire, and pm_{ij} is the probability of the magnetic influence (attracting or repelling) of the *i*th wire (CP) on the *j*th CP.

The average electric current in each wire I_i can be expressed as:

$$(I_{\mathrm{avg}})_{ik} = sign(df_{i,k}) \times \frac{\left| df_{i,k} \right| - df_{\min,k}}{df_{\max,k} - df_{\min,k}}, \tag{19}$$

$$df_{i,k} = fit_k(i) - fit_{k-1}(i), \tag{20}$$

where $df_{i,\mathrm{k}}$ is the variation of the objective function of the *i*th CP in the *k*th movement (iteration). Here, $fit_k(i)$ and $fit_{k-1}(i)$ are the values of the objective function of the *i*th CP at the start of the *k*th and *k-1*th iterations, respectively. Considering absolute values of $df_{i,k}$ for all of the current CPs, $df_{max,k}$ and $df_{min,k}$ will be the maximum and minimum values among these absolute values of *df*, respectively.

A modification can be considered to avoid trapping in part of search space (Local optima) because of attractive electrical force in CSS algorithm [5]

$$F = p_r \times F_E + F_B, \tag{21}$$

where p_r is the probability that an electrical force is a repelling force which is defined as

$$p_{\mathrm{r}} = \begin{cases} 1 & rand > 0.1 \cdot (1 - \mathrm{iter}/\,\mathrm{iter}_{\max}), \\ -1 & \text{else.} \end{cases} \tag{22}$$

where *rand* is a random number uniformly distributed in the range of (0,1), *iter* is the current number of iterations, and $iter_{max}$ is the maximum number of iterations.

Step 2: Making new solutions. Move each CP to the new position and calculate the new velocity as follows:

$$V_{j,new} = \frac{X_{j,new} - X_{j,old}}{\Delta t}, \tag{23}$$

$$X_{j,new} = rand_{j1} \cdot k_a \cdot \frac{F_j}{m_j} \cdot \Delta t^2 + rand_{j2} \cdot k_v \cdot V_{j,old} \cdot \Delta t + X_{j,old}, \tag{24}$$

where $rand_{j1}$ and $rand_{j2}$ are two random numbers uniformly distributed in the range of (0,1). Here, m_j is the mass of the *j*th CP which is equal to q_j. Δt is the time step and is set to unity. k_a is the acceleration coefficient; k_v is the velocity coefficient to control the influence of the previous velocity. k_a and k_v are considered as:

$$\begin{aligned} k_a &= c_1 \cdot \left(1 + \mathrm{iter}/\mathrm{iter}_{\max}\right), \\ k_v &= c_2 \cdot \left(1 - \mathrm{iter}/\mathrm{iter}_{\max}\right), \end{aligned} \tag{25}$$

where c_1 and c_2 are two constants to control the exploitation and exploration of the algorithm, respectively.

Step 3. Position correction of CPs. If each CP violates from its allowable boundary, its position is corrected using harmony search-based approach. In this paper the position correction has been improved and expressed in the next section.

Step 4: CP ranking. Evaluate and compare the values of the fitness function for the new CPs, and sort them in an increasing order.

Step 5: CM updating. If some new CP vectors are better than the worst ones in the CM (means better merit function), include the better vectors in the CM and exclude the worst ones from the CM.

- **Level 3: Controlling the terminating criterion.**

Repeat the search level steps until a terminating criterion is satisfied. The terminating criterion is considered to be the number of iterations.

3.2 Improved version of CSS and MCSS algorithms

In the process of position correction of CPs using harmony search-based approach (Level 2 -

Step 3), the *CMCR* and *PAR* parameters help the algorithm to find globally and locally improved solutions, respectively. *PAR* and *bw* in HS scheme are very important parameters in fine-tuning of optimized solution vectors, and can potentially be useful in adjusting convergence rate of algorithm to optimal solution [12]. The standard version of CSS and MCSS algorithms, use the traditional HS scheme with constant values for both *PAR* and *bw*. Small *PAR* values with large *bw* values can led to poor performance of the algorithm and considerable increase in iterations needed to find optimum solution. Although small *bw* values in final iterations increase the fine-tuning of solution vectors, but in the first iterations *bw* must take a bigger value to enforce the algorithm to increase the diversity of solution vectors. Furthermore, large *PAR* values with small *bw* values usually led to improvement of the best solutions in final iterations a better convergence to optimal solution vector. To improve the performance of the HS scheme and eliminate the drawbacks lies with constant values of *PAR* and *bw*, ICSS and IMCSS algorithms use improved HS scheme with the variable values of *PAR* and *bw* in position correction step. *PAR* and *bw* change dynamically with iteration number as shown in Figure 1 and expressed as follow [12]:

$$PAR(iter) = PAR_{\min} + \frac{(PAR_{\max} - PAR_{\min})}{iter_{\max}} \cdot iter \tag{26}$$

$$bw(iter) = bw_{\max} \exp(c \cdot iter), \tag{27}$$

$$c = \frac{Ln\left(bw_{\min} / bw_{\max} \right)}{iter_{\max}}, \tag{28}$$

where *PAR(iter)* and *bw(iter)* are the values of PAR and bandwidth for current iteration, respectively. bw_{min} and bw_{max} are the minimum and maximum bandwidth, respectively.

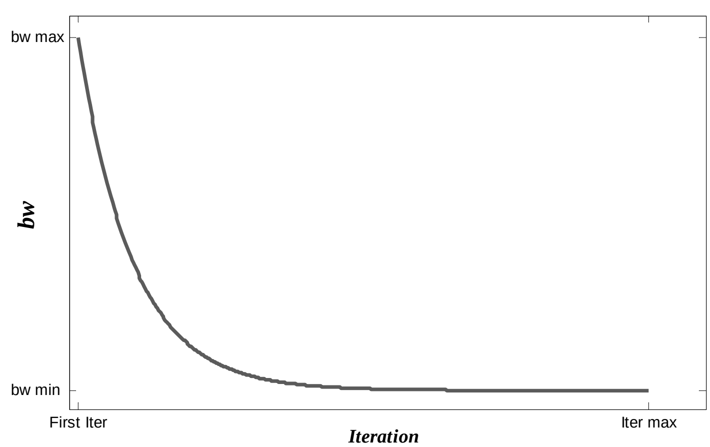

(a)

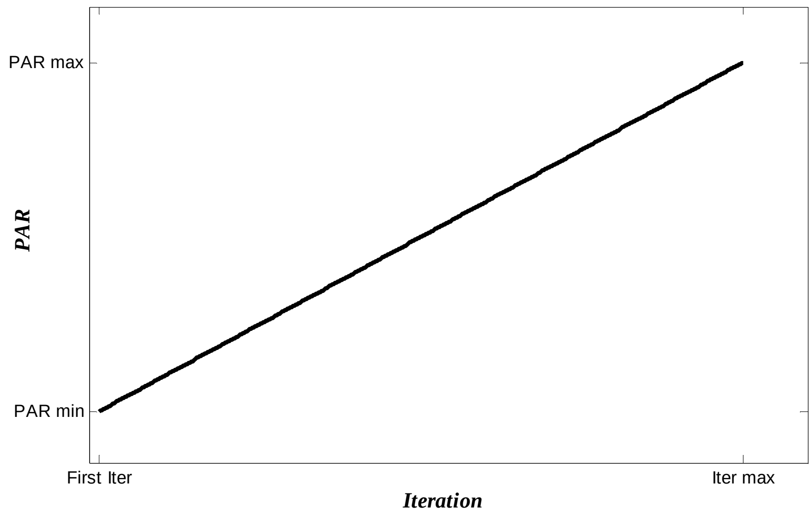

(b)

Figure 1. Variation of (a) bw and (b) PAR versus iteration number

3.3 Discrete ICSS and IMCSS algorithm

The present algorithms can be also applied to optimal design problem with discrete variables. One way to solve discrete problems using a continuous algorithm is to utilize a rounding function which changes the magnitude of a result to the nearest discrete value, as follow

$$X_{j,new} = Fix\left(rand_{j1} \cdot k_a \cdot \frac{F_j}{m_j} \cdot \Delta t^2 + rand_{j2} \cdot k_v \cdot V_{j,old} \cdot \Delta t + X_{j,old} \right), \quad (29)$$

where *Fix(X)* is a function which rounds each elements of vector *X* to the nearest allowable discrete value. Using this position updating formula, the agents will be permitted to select discrete values [13].

4. OPEN APPLICATION PROGRAMMING INTERFACE

The Open Application Programming Interface (OAPI) is a tool that allows users to automate many of the processes required to build, analyze and design models and to obtain customized analysis and design results. It also allows users to link SAP2000 with third-party software, providing a path for two-way exchange of model information with other programs [14]. Most major programming languages can be used to access SAP2000 through the OAPI such as Visual Basic, Visual C# , Intel Visual Fortran, Microsoft Visual C++ , MATLAB and Python.

Kaveh *et. al* [15] have used very this interfacing ability in the form of parallel computing within the Matlab program for practical optimum design of real size 3D steel frames. In this paper the language of technical computing MATLAB is utilized to access SAP2000 through the OAPI and also used for the process of optimization via presented algorithms.

5. STATIC LOADING CONDITIONS

According to ANSI-A58.1 and ASCE/SEI 7-10 codes [16, 17], there are some specific considerations for loading conditions of arched roofs such as barrel vault structures. In this paper, three static loading conditions are considered for optimization of these structures which are expressed as follows:

5.1 Dead load (DL)

A uniform dead load of 100 kg/m^2 is considered for estimated weight of sheeting, space frame, and nodes of barrel vault structure.

5.2 Snow load (SL)

The snow load for arched roofs is calculated according to mentioned codes. Snow loads acting on a sloping surface shall be assumed to act on the horizontal projection of that surface. The sloped roof (balanced) snow load, P_s, shall be obtained by multiplying the flat roof snow load, P_f, by the roof slope factor, C_s, as follows:

$$P_s = C_s . P_f \tag{30}$$

where C_s is

$$C_s = \begin{cases} 1.0 & \alpha < 15^\circ \\ 1.0 - \dfrac{\alpha - 15}{60} & 15^\circ < \alpha < 60^\circ \\ 0.25 & \alpha > 60^\circ \end{cases} \tag{31}$$

The C_s distribution in arched roofs is shown in Figure 2. In this paper, the flat roof snow load P_f is set to 150kg/m^2.

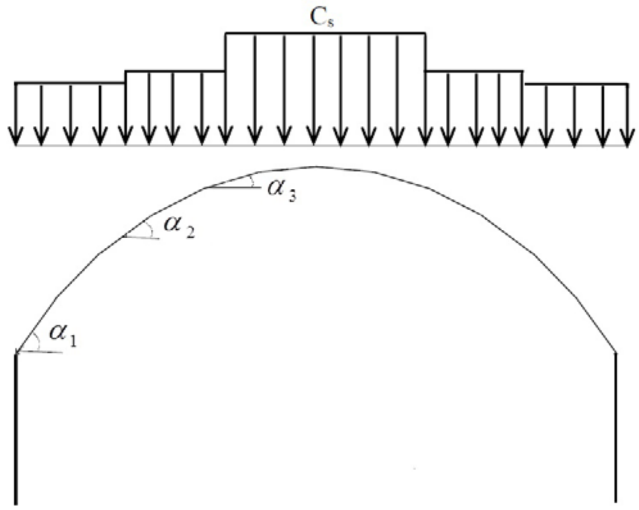

Figure 2. C_s distribution in arched roofs

5.3 Wind load (WL)

For wind load in arched roofs, different loads are applied in the windward quarter, Center half and leeward quarter of the roof which are calculated based on ANSI and ASCE codes [15, 16] as

$$P = q\, G_h\, C_p \tag{32}$$

where q is the wind velocity pressure, G_h is gust-effect factor and C_p is the external pressure coefficient. These parameters are calculated according to ANSI and ASCE codes [15, 16].

6. NUMERICAL EXAMPLES

In this study, two single layer barrel vaults are provided for optimization via proposed algorithm to demonstrate the efficiency of IMCSS algorithm. For all of examples a population of 100 charged particles is used and the value of *CMCR* is set to 0.95. The values of *PARmin* and *PARmax* in IMCSS algorithm are set to 0.35 and 0.9, respectively.

The two examples are discrete optimum design problems and the variables are selected from an allowable set of steel pipe sections taken from AISC-LRFD code [8] shown in Table 1. For analysis of these structures, SAP2000 OAPI is used and the optimization process is performed in MATLAB.

In all examples, the material density is 0.2836 lb/in^3 (7850 kg/m^3) and the modulus of elasticity is 30450 ksi (2.1×10^6 kg/cm^2). The yield stress F_y of steel is taken as 34135.96 psi (2400 kg/cm^2) for both problems.

Table 1: The allowable steel pipe sections taken from AISC-LRFD code [8]

Number		Section Name	Weight per ft (lb)	Area (in)
1	Standard Weight	P0.5	0.85	0.25
2		P0.75	1.13	0.333
3		P1	1.68	0.494
4		P1.25	2.27	0.669
5		P1.5	2.72	0.799
6		P10	3.65	1.07
7		P12	5.79	1.7
8		P2	7.58	2.23
9		P2.5	9.11	2.68
10		P3	10.79	3.17
11		P3.5	14.62	4.3
12		P4	18.97	5.58
13		P5	28.55	8.4
14		P6	40.48	11.9
15		P8	49.56	14.6
16	Extra Strong	XP0.5	1.09	0.32
17		XP0.75	1.47	0.433
18		XP1	2.17	0.639
19		XP1.25	3	0.881
20		XP1.5	3.63	1.07
21		XP10	5.02	1.48
22		XP12	7.66	2.25
23		XP2	10.25	3.02
24		XP2.5	12.5	3.68
25		XP3	14.98	4.41
26		XP3.5	20.78	6.11
27		XP4	28.57	8.4
28		XP5	43.39	12.8
29		XP6	54.74	16.1
30		XP8	65.42	19.2
31	Double-Extra Strong	XXP2	9.03	2.66
32		XXP2.5	13.69	4.03
33		XXP3	18.58	5.47
34		XXP4	27.54	8.1
35		XXP5	38.59	11.3
36		XXP6	53.16	15.6
37		XXP8	72.42	21.3

6. 1 A 173-Bar Single Layer Barrel Vault Frame

The 173-bar single layer barrel vault frame which has a 2-way grid shown in Figure 3. The geometry of this structure is taken from Ref. [6].

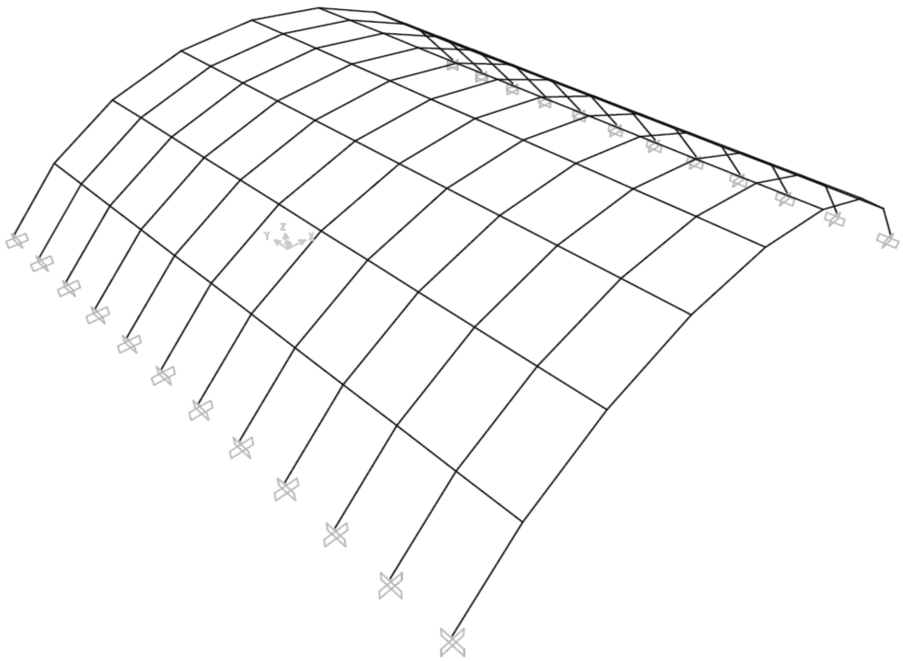

(a)

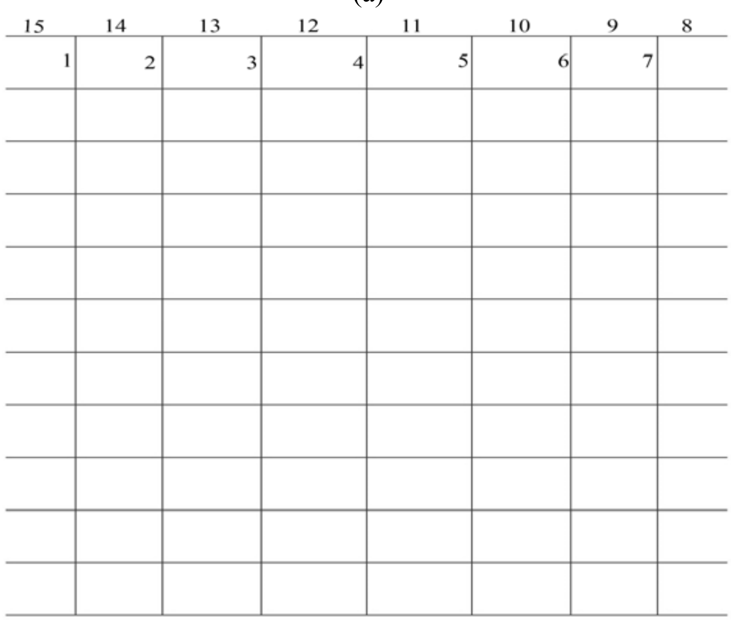

(b)

Figure 3. The 173-bar single layer barrel vault frame, (a) 3-dimensional view, (b) Member groups in top view

This spatial structure consists of 108 joints and 173 members. As seen in Figure 3 (b), all members of this structure are categorized into 15 groups. The nodal displacements are limited to ±1.05 in (26 mm) in x, y directions and ±1.64 in (41 mm) in z direction.

The configuration of the 173-bar single layer barrel vault is as follows:

- Span (S) =30 m (1181.1 in)
- Height (H) =8 m (314.96 in)
- Length (L) = 30 m (1181.1 in)

This spatial structure is subjected to three loading conditions according to considerations mentioned in Section 5:

A uniform dead load of 100 kg/m^2 is applied on the roof. The applied snow and wind loads on this barrel vaults are shown in Figures 4 (a) and (b), respectively.

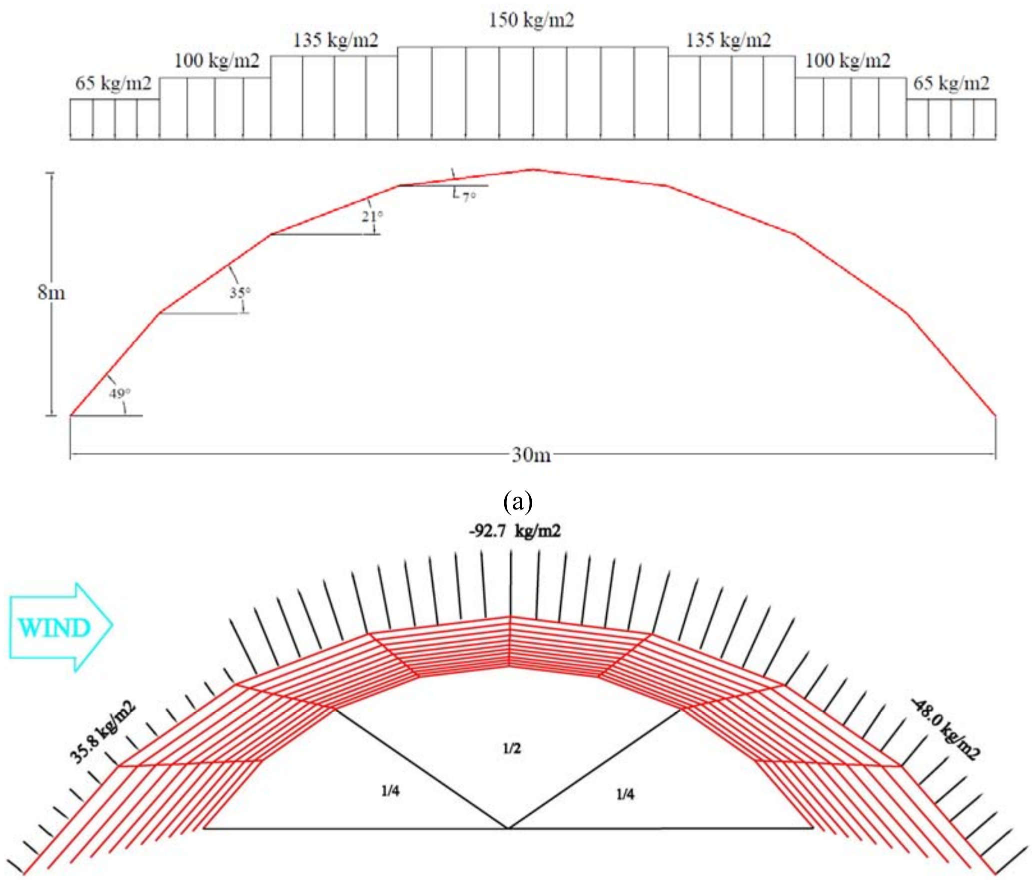

(a)

(b)

Figure 4. The 173-bar single layer barrel vault frame subjected to: (a) Snow loading, (b) Wind loading

Figure 5 shows the convergence history for optimization of this structure using MCSS and IMCSS algorithms. The comparison of the optimal design results using presented algorithms is provided in Table 2.

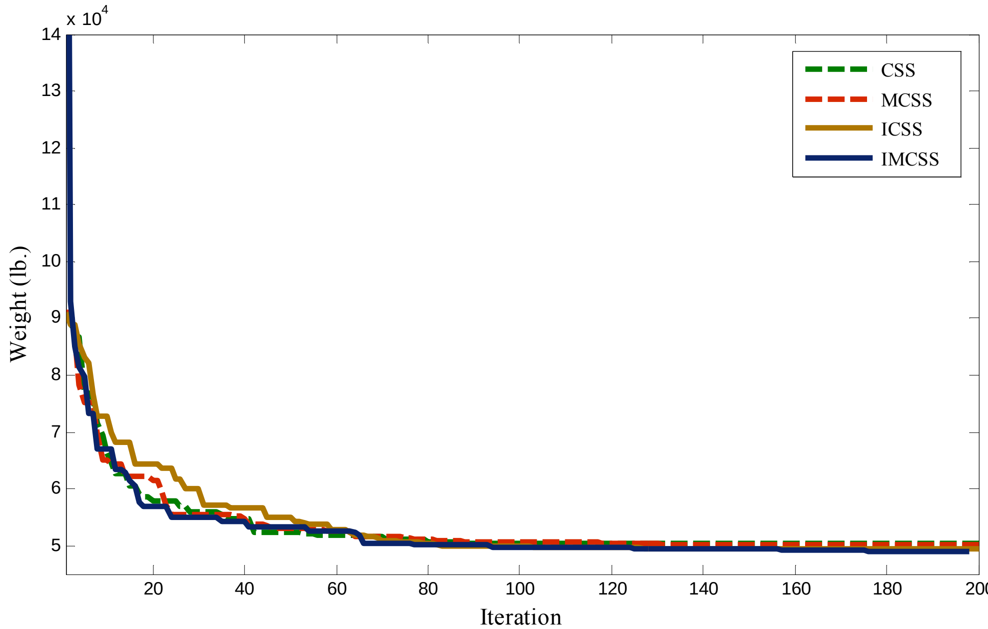

Figure 5. Convergence history for the 173-bar single layer barrel vault frame using CSS, MCSS, ICSS and IMCSS algorithms

Table 2: Optimal design comparison for the 173-bar single layer barrel vault frame (in^2)

Element group	Optimal sections and cross-sectional areas (in^2)							
	CSS		MCSS		ICSS		IMCSS	
	Section Name	Area (in^2)	Section Name	Area (in^2)	Section Name	Area (in^2)	Section Name	Area (in^2)
1	'P1'	0.494	'XP1'	0.639	'P0.5'	0.25	'P0.5'	0.25
2	'P1'	0.494	'XP0.75'	0.433	'P0.5'	0.25	'P0.5'	0.25
3	'XP1.5'	1.07	'P1'	0.494	'P0.5'	0.25	'P0.5'	0.25
4	'P0.75'	0.333	'P0.75'	0.333	'P0.5'	0.25	'P0.5'	0.25
5	'XP0.5'	0.32	'XP1'	0.639	'P0.5'	0.25	'XP0.5'	0.32
6	'XP1.25'	0.881	'XP1.5'	1.07	'P0.5'	0.25	'XP0.5'	0.32
7	'P1.5'	0.799	'XP1'	0.639	'P0.5'	0.25	'P0.5'	0.25
8	'P10'	11.9	'P10'	11.9	'P10'	11.9	'P12'	14.6
9	'P10'	11.9	'P10'	11.9	'P10'	11.9	'XP6'	8.4
10	'P10'	11.9	'P10'	11.9	'P10'	11.9	'P10'	11.9
11	'P10'	11.9	'P10'	11.9	'P10'	11.9	'P10'	11.9
12	'P10'	11.9	'P10'	11.9	'P10'	11.9	'P10'	11.9
13	'P6'	5.58	'P6'	5.58	'P6'	5.58	'P6'	5.58
14	'P6'	5.58	'P6'	5.58	'P6'	5.58	'P6'	5.58
15	'P10'	11.9	'P10'	11.9	'P10'	11.9	'P10'	11.9
Weight. lb.	50295.90		50247.66		49411.27		48985.05	
Weight. Kg.	22813.84		22791.96		22412.58		22219.24	
Max. Disp. Ratio	0.8196		0.8196		0.8196		0.9051	
Max. Strength Ratio	0.8724		0.8689		0.8695		0.8751	
No. of analyses	20,000		20,000		20,000		19,800	

As seen in Table 2, the IMCSS algorithm finds the best solutions in 198 iterations (19,800 analyses), but the CSS, MCSS and ICSS algorithms didn't obtain any better solutions in 20,000 analyses. The best weights of IMCSS is 48985.05 lb (22219.24 kg), while it is 50295.90 lb, 50247.66 lb and 49411.27 lb for the CSS, MCSS and ICSS algorithms, respectively. As it can be seen in the results, the IMCSS algorithm gives a better weight in a lower number of analyses than other algorithms. Also, it can be seen in the results of Table 2, the maximum strength ratio for CSS, MCSS, ICSS and IMCSS algorithms is 0.8724, 0.8689, 0.8695 and 0.8751, respectively, and the maximum displacement ratio is 0.9051 for IMCSS and is 0.8196 for CSS, MCSS and ICSS algorithms.

Figures 6(a) to 6(d) provide strength ratios for all elements of the 173-bar single layer barrel vault frame for optimal results of CSS, MCSS, ICSS and IMCSS algorithms, respectively. As shown in all these figures, the strength ratios of elements are lower than 1, thus there is no violation of stress constraints in the optimal results of proposed algorithms for this structure and all constraints are satisfied. Also, the maximum strength ratios for element groups of the 173-bar single layer barrel vault frame are provided in Figures 7(a) and 7(b) for optimal results of ICSS and IMCSS algorithms, respectively.

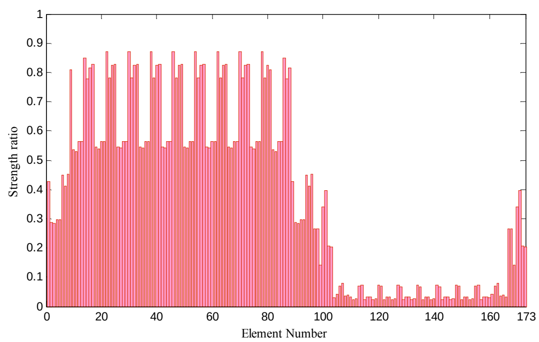

(a)

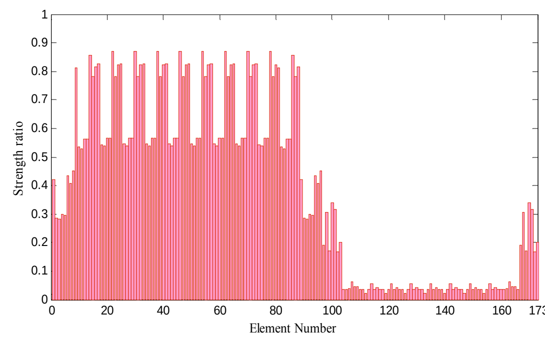

(b)

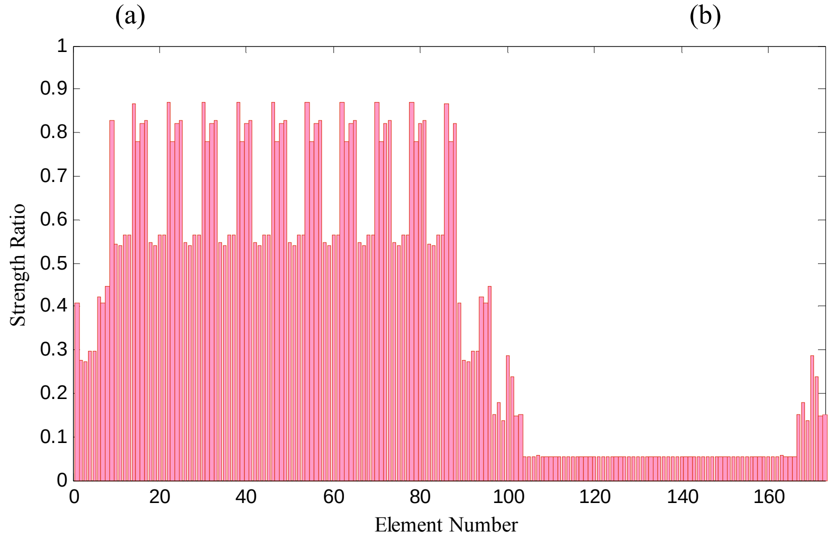

(c)

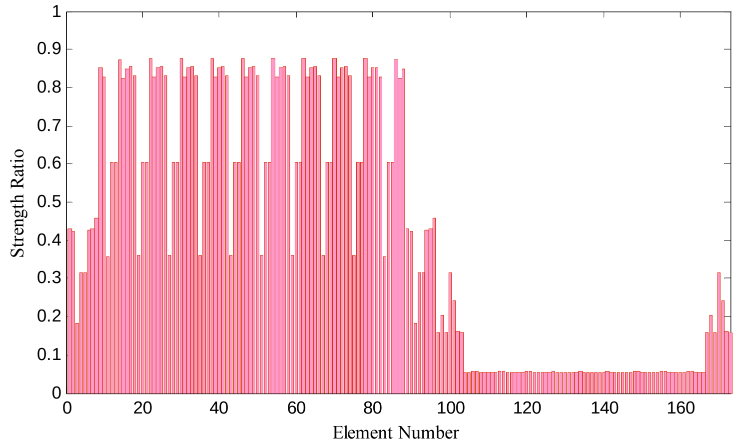

(d)

Figure 6. Strength ratios for the elements of the 173-bar single layer barrel vault frame for optimal results of (a) CSS, (b) MCSS, (c) ICSS and (d) IMCSS algorithms

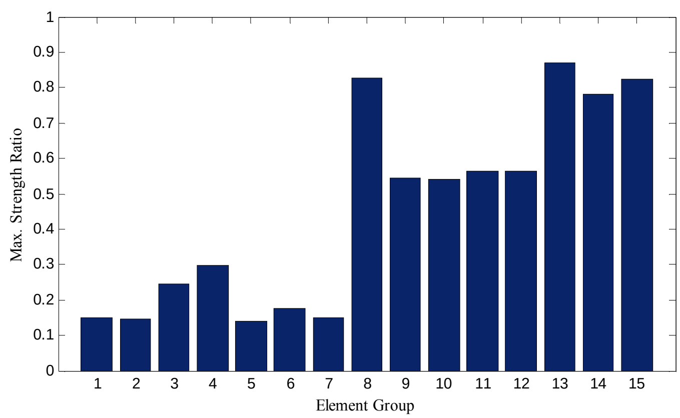

(a)

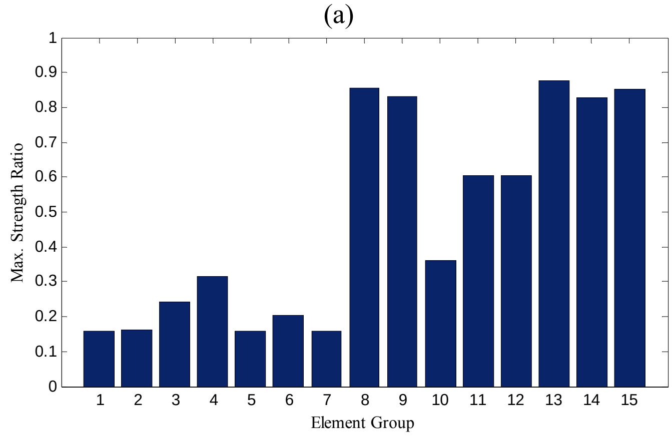

(b)

Figure 7. Maximum strength ratios for element groups of the 173-bar single layer barrel vault frame for optimal results of (a) ICSS and (b) IMCSS algorithms

6. 2 A 292-Bar Single Layer Barrel Vault

This single layer barrel vault which has a three-way pattern is shown in Figure 8. This structure consists of 117 joints and 292 members. Considering the symmetry of the barrel vault and loading condition, all members are grouped into 30 independent size variables groups as shown in Figures 8(b). The nodes are subjected to the displacement limits of ±1.31 in (33 mm) in x, y directions and ±1.97 in (50 mm) in z directions.

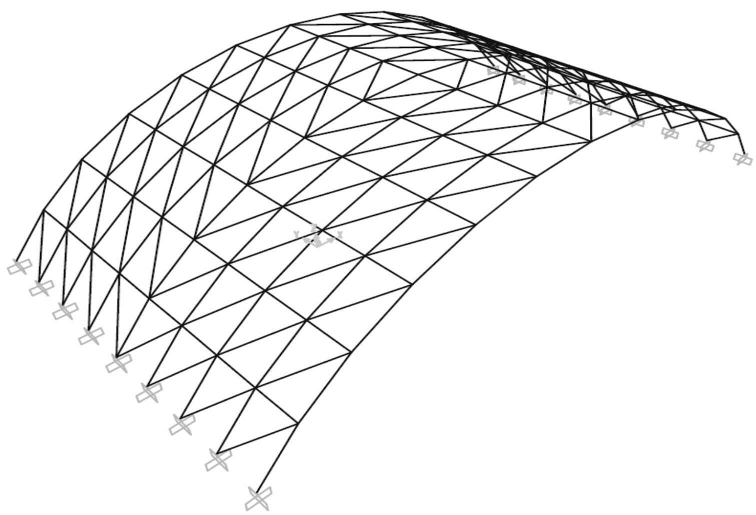

(a)

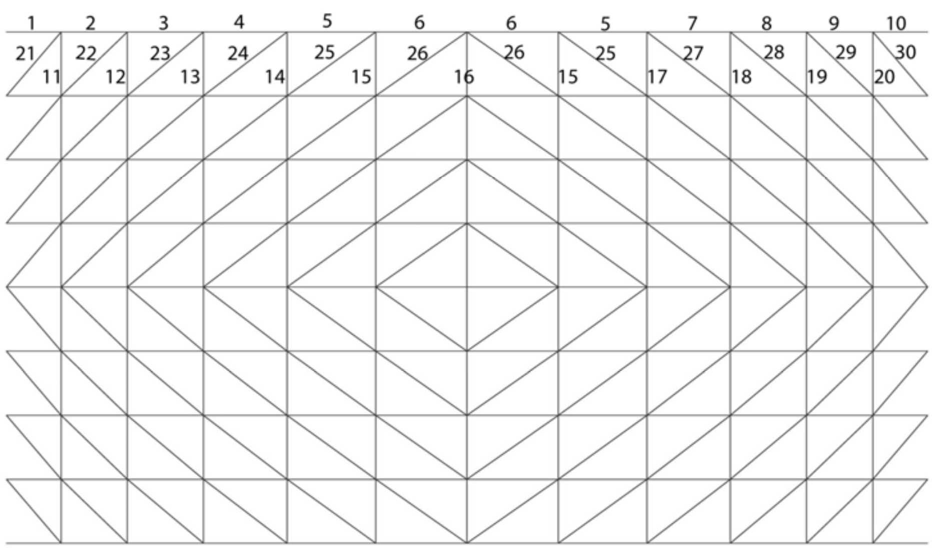

(b)

Figure 8. The 292-bar single layer barrel vault frame: (a) 3-dimensional view, (b) Member groups in top view

The configuration of the 292-bar single layer barrel vault is as follows

- Span (S) =36 m (1417.3 in)
- Height (H) =8 m (393.7 in)
- Length (L) = 20 m (787.4 in)

According to loading considerations mentioned in Section 5, this barrel vault is subjected to three loading conditions as follows:

A uniform dead load of 100 kg/m^2 is applied on the roof. The applied snow load and wind load acting on this barrel vaults is shown in Figures 9 (a) and (b), respectively.

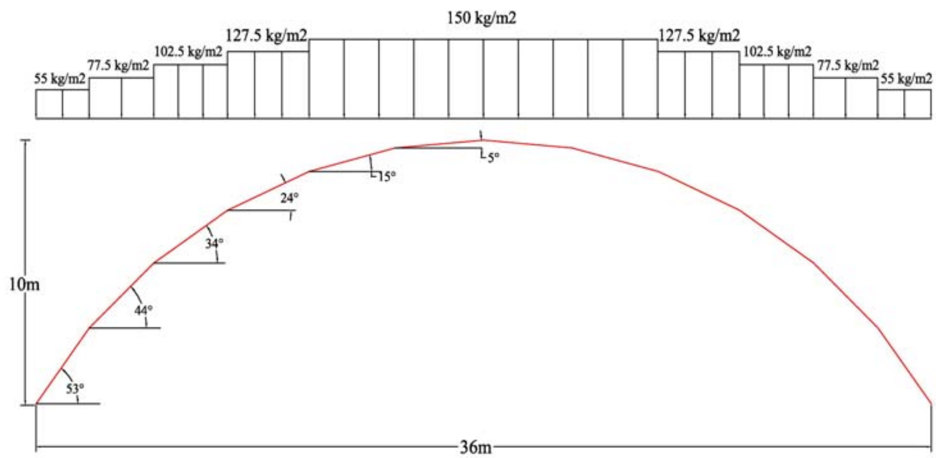

(a)

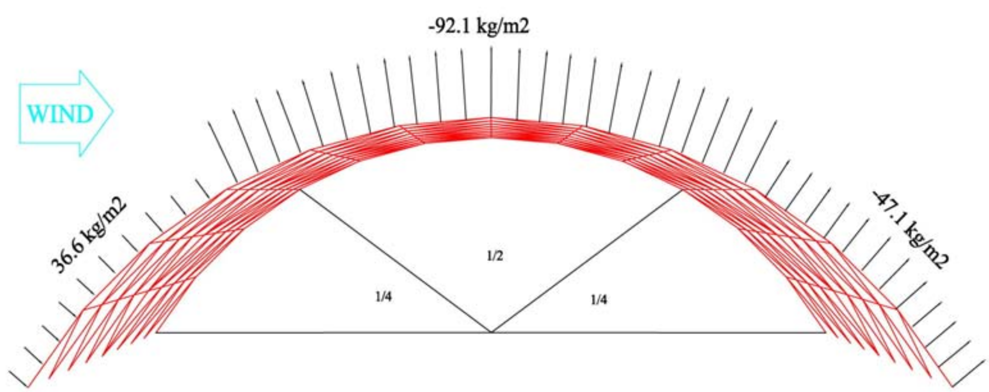

(b)

Figure 9. The 292-bar single layer barrel vault frame subjected to: (a) Snow loading, (b) Wind loading

Table 3 draws a comparison among the results of the CSS, MCSS, ICSS and IMCSS algorithms for this structure. The convergence history of the algorithms is shown in Figure 10.

Table 3: Optimal design comparison for the 292-bar single layer barrel vault (in^2)

Element group	Optimal sections and cross-sectional areas (in.2)							
	CSS		MCSS		ICSS		IMCSS	
	Section Name	Area (in^2)	Section Name	Area (in^2)	Section Name	Area (in^2)	Section Name	Area (in^2)
1	'P12'	14.6	'P12'	14.6	'P10'	11.9	'P12'	14.6
2	'P10'	11.9	'XP6'	8.4	'P10'	11.9	'XP6'	8.4
3	'XP8'	12.8	'XP8'	12.8	'P12'	14.6	'P10'	11.9
4	'P6'	5.58	'P12'	14.6	'XP8'	12.8	'XP6'	8.4
5	'XP8'	12.8	'P10'	11.9	'P10'	11.9	'P10'	11.9
6	'P10'	11.9	'P10'	11.9	'P10'	11.9	'P10'	11.9
7	'P10'	11.9	'P12'	14.6	'P10'	11.9	'P10'	11.9
8	'P12'	14.6	'XP10'	16.1	'P10'	11.9	'P12'	14.6
9	'P10'	11.9	'P10'	11.9	'P10'	11.9	'P10'	11.9
10	'XP12'	19.2	'XP12'	19.2	'XP12'	19.2	'P12'	14.6
11	'XP2.5'	2.25	'P0.5'	0.25	'P1.25'	0.669	'XP2'	1.48
12	'P1.25'	0.669	'XP0.75	0.433	'XP2'	1.48	'P1.5'	0.799
13	'XP5'	6.11	'P2.5'	1.7	'P1'	0.494	'P1.25'	0.669
14	'XP3.5'	3.68	'XP1'	0.639	'XP2'	1.48	'P1.5'	0.799
15	'P2.5'	1.7	'P1.25'	0.669	'XP1.5'	1.07	'P1'	0.494
16	'P4'	3.17	'XP1.5'	1.07	'XP1.5'	1.07	'P1.5'	0.799
17	'XP2'	1.48	'P3.5'	2.68	'P1.5'	0.799	'XP2.5'	2.25
18	'XP2'	1.48	'XP1.5'	1.07	'XP2'	1.48	'P1.25'	0.669
19	'XXP3'	5.47	'XP1'	0.639	'XP1'	0.639	'XP1'	0.639
20	'P5'	4.3	'P3'	2.23	'XP1.25	0.881	'XP2'	1.48
21	'XXP2'	2.66	'XP2'	1.48	'XP3'	3.02	'P1.5'	0.799
22	'XP2.5'	2.25	'XP1.5'	1.07	'XP2'	1.48	'XP1.5'	1.07
23	'XP1'	0.639	'P3'	2.23	'XP0.75	0.433	'P1.5'	0.799
24	'XP2'	1.48	'P2.5'	1.7	'XP0.75	0.433	'XP1.5'	1.07
25	'P1.5'	0.799	'P1.25'	0.669	'XP1.25	0.881	'P1.25'	0.669
26	'XP1.5'	1.07	'P1.25'	0.669	'XP1.25	0.881	'XP1.25	0.881
27	'P1.5'	0.799	'P2.5'	1.7	'P1.5'	0.799	'P1.5'	0.799
28	'XP2'	1.48	'P3'	2.23	'XP1.25	0.881	'P1.5'	0.799
29	'XP1.5'	1.07	'P1.5'	0.799	'XP2'	1.48	'XP2'	1.48
30	'P3.5'	2.68	'P1.5'	0.799	'P4'	3.17	'XP8'	12.8
Weight. lb.	68324.57		65892.33		63694.69		62968.19	
Weight. Kg.	30991.50		29888.26		28891.43		28561.89	
Max. Disp. Ratio	0.7986		0.9013		0.9387		0.7882	
Max. Strength Ratio	0.9527		0.8883		0.9595		0.9939	
No. of analyses	20,000		20,000		20,000		17,500	

Table 3 shows that, the best weights of IMCSS algorithm is 62968.19 lb. (28561.89 kg), while it is 68324.57 lb, 65892.33 and 63694.69 lb for the CSS, MCSS and ICSS algorithms. The IMCSS algorithm finds the best solutions in 175 iterations (17,500 analyses), but other algorithms didn’t find any better solution in 20,000 analyses.

Also, Table 3 shows the maximum displacement and strength ratios for all algorithms. The values of maximum strength ratio for CSS, MCSS, ICSS and IMCSS algorithms are 0.9527, 0.8883, 0.9595 and 0.9939, respectively, and for the maximum displacement ratio, the values are 0.7986, 0.9013, 0.9387 and 0.7882, respectively.

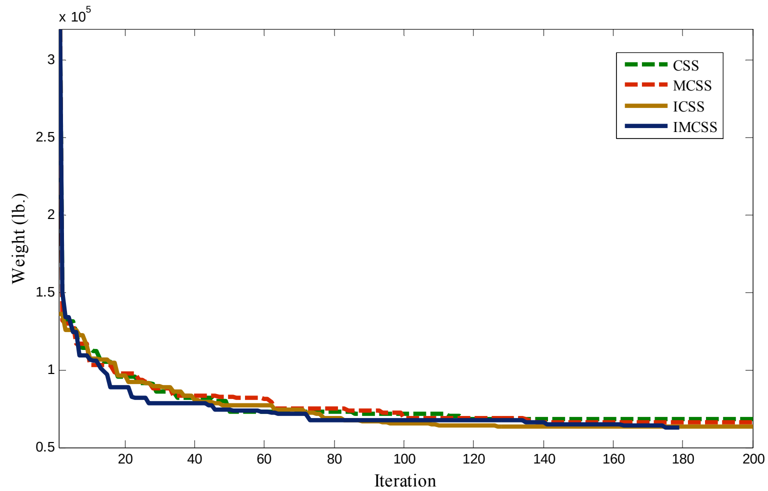

Figure 10. Convergence history for the 292-bar single layer barrel vault frame using MCSS and IMCSS algorithms

The strength ratios for all elements of the 292-bar single layer barrel vault frame for optimal results of all presented algorithms, are provided in Figure 11(a) through (d).

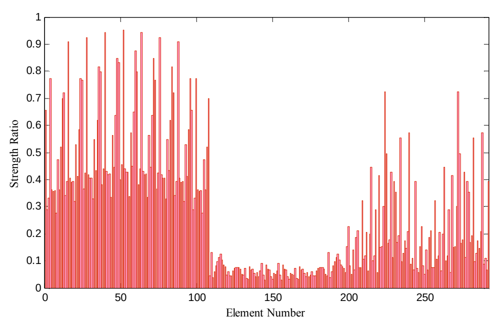

(a)

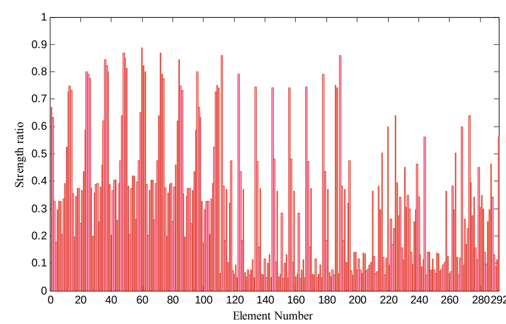

(b)

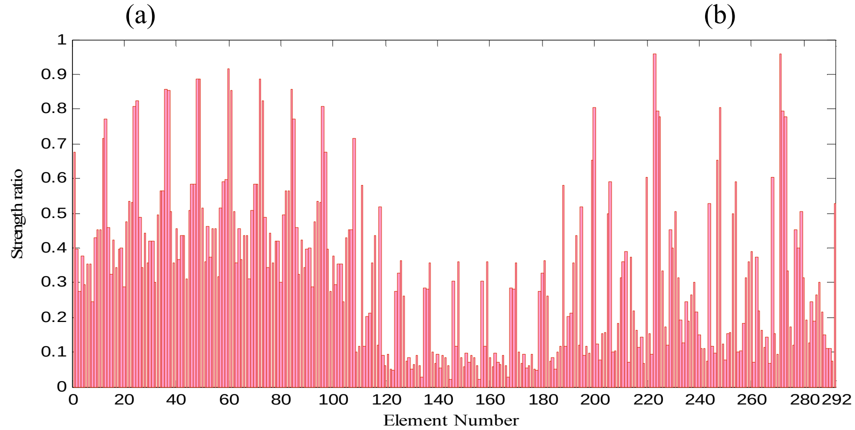

(c)

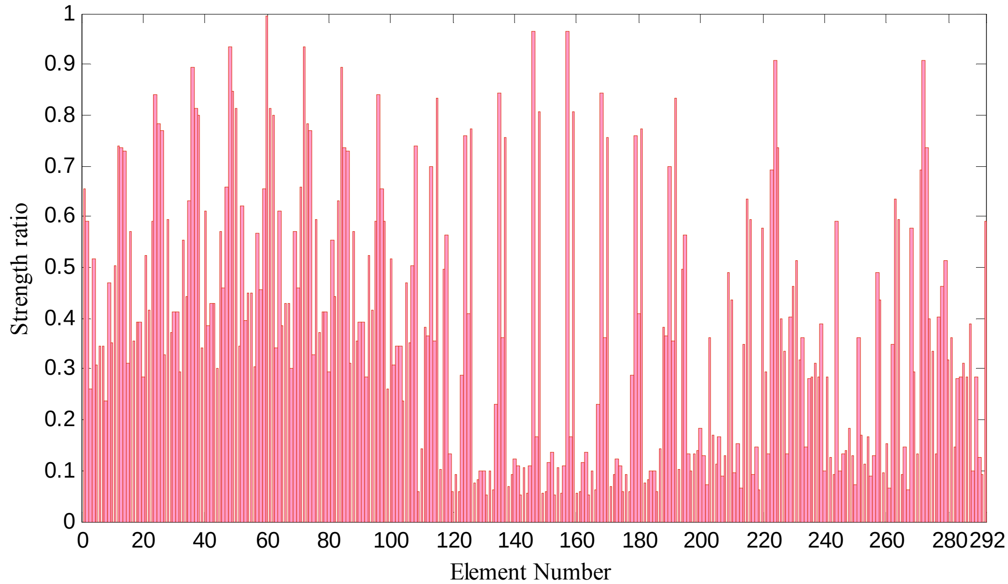

(d)

Figure 11. Strength ratios for the elements of the 292-bar single layer barrel vault frame for optimal results of (a) CSS, (b) MCSS, (c) ICSS and (d) IMCSS algorithms

and the maximum strength ratios for element groups of the 173-bar single layer barrel vault frame are provided in figures 12(a) and (b) for optimal results of ICSS and IMCSS algorithms, respectively.

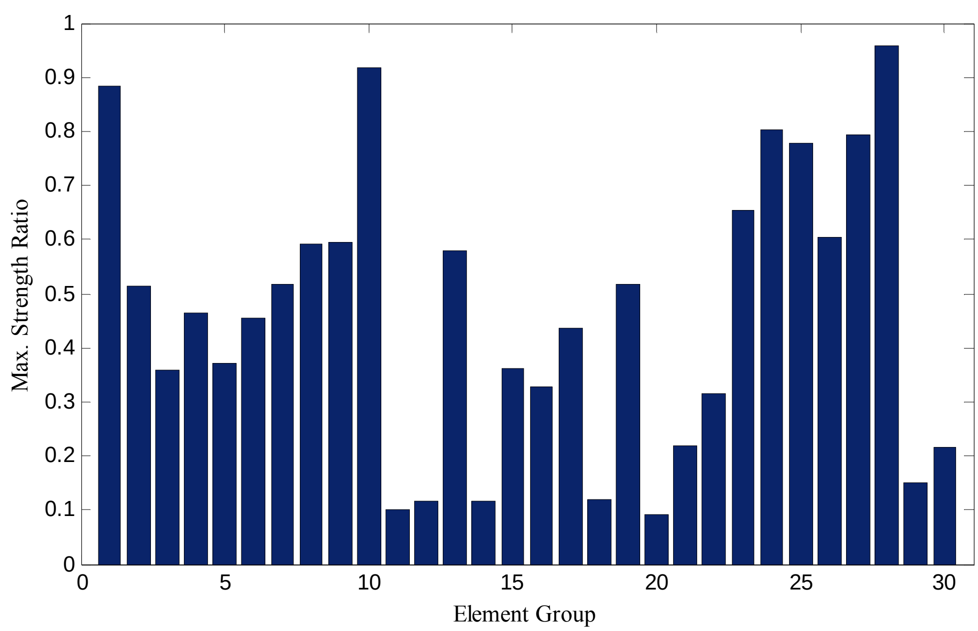

(a)

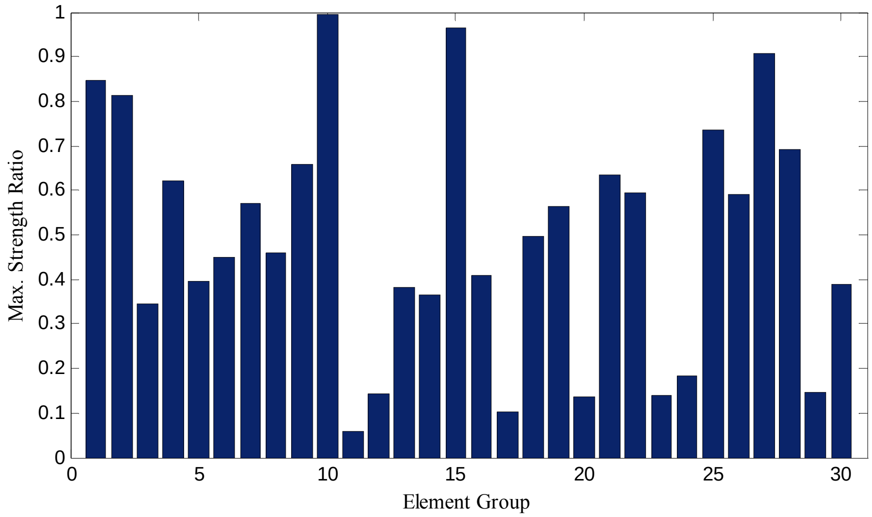

(b)

Figure 12. Maximum strength ratios for element groups of the 292-bar single layer barrel vault frame for optimal results of; (a) ICSS and (b) IMCSS algorithms

As shown in figures 11(a) and 11(b), all of strength ratios of elements are lower than 1, therefore, all of presented algorithms have no violation of constraints in their best solutions and all constraints are reasonably satisfied.

6. CONCLUSIONS

This paper has employed an improved magnetic charged system search (IMCSS) and an open application programming interface (OAPI) for optimization of single layer barrel vaults to demonstrate the ability of the proposed approach for optimization of practical barrel vault structures.

The open application programming interface (OAPI) is utilized in the process of structural analysis to link the analysis software with the programming language. In IMCSS algorithm, for achieving better convergence rate and optimal results, an improved harmony search scheme is used for position correction of CPs, and two of the most important parameters (PAR and bw) of the algorithm are improved.

In this study, two single layer barrel vault frames with different patterns are optimized via the proposed algorithm. In this process, to achieve a more realistic model of the structures, the valid codes of ANSI and ASCE are used for modeling static loading conditions acting on the structures.

As it can be seen in comparison the results of all presented algorithms for both numerical examples, IMCSS has found more optimal values for the weight of structures than other algorithms. The results also demonstrated the robustness of the proposed algorithm in achieving the best solutions in a lower number of analyses than MCSS algorithm. Also, it can be concluded that the OAPI is a powerful interface tool for the process of structural analysis in optimal design of practical and realistic large scale barrel vaults.

REFERENCES

1. Makowski ZS. *Analysis, Design and Construction of Braced Barrel Vaults*, Taylor & Francis, 2006.
2. Ramaswamy GS, Eekhout M, Suresh GR. *Analysis, Design and Construction of Steel Space Frames,* Thomas Telford Publishing, 2002.
3. Subramanian N. *Principles of Space Structures,* 2nd edition, Wheeler Publishing, 1999.
4. Kaveh A, Talatahari S. A novel heuristic optimization method: Charged system search, *Acta Mech*, 2010; **213**(3-4): 267–89.
5. Kaveh A, Motie Share MA, Moslehi M. Magnetic charged system search: a new meta-heuristic algorithm for optimization, *Acta Mech,* 2013; **224**(1): 85–107.
6. Kaveh A, Eftekhar B. Improved Big Bang Big Crunch to Optimize Barrel Vault Frames, *Proceeding of the 9th International Congress on Civil Engineering*, Isfahan University of Technology (IUT), Isfahan, Iran, 2012.
7. Kaveh A, Farahani M, Shojaei N. Optimal design of barrel vaults using charged search system, *Int J Civil Eng,* 2012; **10**(4)**:** 301–08.
8. American Institute of Steel Construction (AISC). *Steel Construction Manual*, 13th edition, Chicago, Illinois, USA, 2005.
9. British Standards Institution (BSI). *Structural use of Steelwork in building Part 1: Code of Practice for Design-Rolled and Welded Section (BS5950-1)*, British Standards Institution, London, UK, 2000.
10. Kameshki ES, Saka MP. Optimum geometry design of nonlinear braced domes using genetic algorithm, *Comput Struct*, 2007; **85**: 71–9.
11. Kaveh A, Farahmand Azar B, Talatahari S. Ant colony optimization for design of space trusses, *Int J Space Struct*, 2008; **23**(3): 167–81.
12. Mahdavi M, Fesanghary M, Damangir E. An improved harmony search algorithm for solving optimization problems, *Appl Math Comput*, 2007; **188**:1567–79.
13. Kaveh A, Talatahari S. A charged system search with a fly to boundary method for discrete optimum design of truss structures, *Asian J Civil Eng*, 2010; **11**(3): 277–29.
14. Computers and Structures Inc. (CSI). *SAP2000 OAPI Documentation*, University of California, Berkeley, California 2011.
15. Kaveh A, Bakhshpoori T, Ashoory M. An efficient optimization procedure based on cuckoo search algorithm for practical design of steel structures, *Int J Optim Civil Eng,* 2012; 2(1): 1-14.

16. American National Standards Institute (ANSI). *Minimum Design Loads for Buildings and Other Structures* (ANSI A58.1), 1980.
17. American Society of Civil Engineers (ASCE). *Minimum Design Loads for Buildings and Other Structures* (ASCE-SEI 7-10), 2010.